



Topological metadefects: tangles of dislocations

Pawel Pieranski, Mehdi Zeghal, Maria Helena Godinho, Patrick Judeinstein,
Rémi Bouffet-Klein, Bastien Liagre, Nicodème Rouger

► To cite this version:

Pawel Pieranski, Mehdi Zeghal, Maria Helena Godinho, Patrick Judeinstein, Rémi Bouffet-Klein, et al.. Topological metadefects: tangles of dislocations. *Physical Review Letters*, 2023, 131 (12), pp.128101. 10.1103/PhysRevLett.131.128101 . hal-04227180

HAL Id: hal-04227180

<https://hal.science/hal-04227180>

Submitted on 3 Oct 2023

HAL is a multi-disciplinary open access archive for the deposit and dissemination of scientific research documents, whether they are published or not. The documents may come from teaching and research institutions in France or abroad, or from public or private research centers.

L'archive ouverte pluridisciplinaire **HAL**, est destinée au dépôt et à la diffusion de documents scientifiques de niveau recherche, publiés ou non, émanant des établissements d'enseignement et de recherche français ou étrangers, des laboratoires publics ou privés.

Topological metadefects : tangles of dislocations

Pawel Pieranski* and Mehdi Zeghal

Université Paris-Saclay, Laboratoire de Physique des Solides, 91405 Orsay, France

Maria Helena Godinho

i3N/CENIMAT, Department of Materials Science,
NOVA School of Science and Technology, NOVA University Lisbon,
Campus de Caparica, Caparica 2829 - 516, Portugal

Patrick Judeinstein

Université Paris-Saclay, CEA, CNRS, LLB, 91191 Gif-sur-Yvette, France

Rémi Bouffet-Klein, Bastien Liagre and Nicodème Rouger

ENS Paris-Saclay, 4 avenue des Sciences, 91190 Gif-sur-Yvette, France

(Dated: 9 août 2023)

The concept of topological defects is universal. In condensed matter, it applies to disclinations, dislocations or vortices that are fingerprints of symmetry breaking during phase transitions. Using as a generic example the tangles of dislocations, we introduce the concept of topological metadefects i.e. defects made of defects. We show that in cholesterics, dextrogyre and levogyre primary tangles are generated through the $D_2 \rightarrow C_2$ symmetry breaking from the coplanar dislocation pair called Lehmann cluster submitted to a high enough tensile strain. The primary tangles can be wound up individually into double-helices. They can also annihilate in pairs or associate into tangles of higher orders following simple algebraic rules.

Topological defects such as vortices, dislocations or disclinations are fingerprints of order parameters resulting from broken symmetries [1, 2]. Here, we introduce the new concept of topological defects of a higher order, that we propose to call *metadefects*, using as a generic example tangles of dislocations in cholesterics.

Today, in the light of experiments reported below, we can say that such tangles certainly occur frequently in the well known textures of cholesteric liquid crystals called oily streaks, which are networks of clusters of dislocations but formerly, as far as we know, they have not been recognised and discussed explicitly. For the sake of simplicity, we present here the first evidence of tangles produced in a controlled manner from the so-called Lehmann clusters [3–6]. The letter is organised as follows :

1. First, we explain what is the *Lehmann cluster* and how it can be obtained by a *collision of two parallel dislocations* with opposite Burgers vectors $b = p_o$ and $b = -p_o$ (p_o is the full 2π pitch of the cholesteric helix).
2. Subsequently, we introduce the *overlapping instability* of the Lehmann cluster submitted to a high enough tensile strain and explain how the corresponding $D_2 \rightarrow C_2$ symmetry breaking produces one or more *primary tangles*.
3. Next, we show that the primary tangles resulting from the overlapping instability can be wound up into *dextrogyre* or *levogyre double-helices* [7–10].

4. Finally, we point out that several textures in cholesterics observed or discussed formerly [6, 11–13] can also be interpreted as topological metadefects.

Our experiments were made with cholesteric droplets confined by capillarity between two crossed cylindrical mica sheets (see Fig.1a and also ref. [12]). The radius R_m of curvature of mica sheets is of the order of 150mm and the initial minimal distance h_{min} of the gap is of the order of 10 cholesteric pitches $p_o \approx 18\mu\text{m}$. When the radius r_d of droplets is of the order of 1mm , the thickness of the gap which varies with the distance r from the centre as

$$h(r) = h_{min} + r^2/(2R_m) \quad (1)$$

increases only by $3\mu\text{m}$ from the centre to the meniscus ($r = r_d$) which is much less than the pitch p_o . For this reason, in experiments discussed below, variation of the thickness $h(r)$ with r can be neglected.

The series of four pictures in Figs.1d-g shows evolution of two dislocation loops with $N+1$ cholesteric pitches nucleated previously by a tensile strain in a droplet containing $N = 8$ full cholesteric pitches (point 1 in Fig.2a). Upon the action of the Peach-Koehler force

$$\tilde{F}_{PK} = \frac{F_{PK}}{\frac{2K_{22}\pi^2}{p_o}} = \left(1 - \frac{N+1/2}{\tilde{h}}\right) \quad (2)$$

corresponding to $\tilde{h} = h/p_o = 9$ (point 2 in Fig.2a), the two dislocation loops expand and collide (K_{22} is the Frank-Oseen coefficient for the twist distortion). At first sight, one could expect that the collision of two dislocations should result in their coalescence (or rewiring). Surprisingly, this is not the case in the experiment repre-

* pawel.pieranski@u-psud.fr

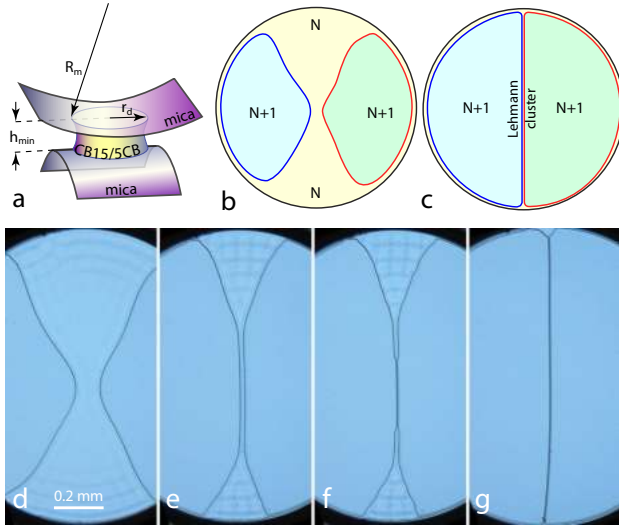


FIGURE 1. Generation of the Lehmann cluster. a) Geometry of the experiment : a cholesteric droplet confined by capillarity between crossed cylindrical mica sheets (for a better visual readability, the thickness h_{min} of the gap is exaggerated). b) Expanding coplanar dislocation loops. c) Lehmann cluster resulting from the collision of the expanding loops. d-g) Generation of the Lehmann cluster by collision of the expanding coplanar dislocation loops. (0.87% CB15/5CB, $N=8$, $p_o = 18\mu m$, $h_{min} = 9p_o$, point 2 in Fig.2a)

sented in Figs.1e-g where the collision of the two loops results in the association of dislocations into the Lehmann cluster (see the video *Lehmann cluster* of Supplementary Materials).

The coalescence of the colliding coplanar loops is avoided because as it was pointed out by Smalyukh and Lavrentovich [4] the Lehmann cluster is the most stable state of a pair of dislocations with the opposite Burgers vectors (see Fig.2f); its energy per unit length (tension) T_{LC} is smaller than the total energy $2T$ of the two dislocations before their association. This is obvious in the experiment represented in Fig.2b where the two dislocations connected to the Lehmann cluster form the angle $\alpha = 80^\circ$. From the condition of the equilibrium of tensions $T_{LC} = 2T \cos(\alpha/2)$ one obtains $T_{LC}/(2T) = 0.77$. (**Warning** : The cholesteric phase is continuous; the dotted lines in Figs.2 f, j and k delimit quasi-layers in which molecules rotate by 2π .)

After its generation, the Lehmann cluster is submitted to a higher tensile strain ($\tilde{h} = h/p_o \approx 10.3$, point 3 in Fig.2a) triggering the overlapping instability that we will discuss in more details below. Here, the overlapping instability splits extremities of the Lehmann cluster into pairs of dislocations delimiting triangular fields labeled “N+2 overlap” shown in Figs.2b and h. Subsequently, the splitting of the Lehmann cluster progresses until the vertices A and B of the triangular fields collide at the center t of the droplet.

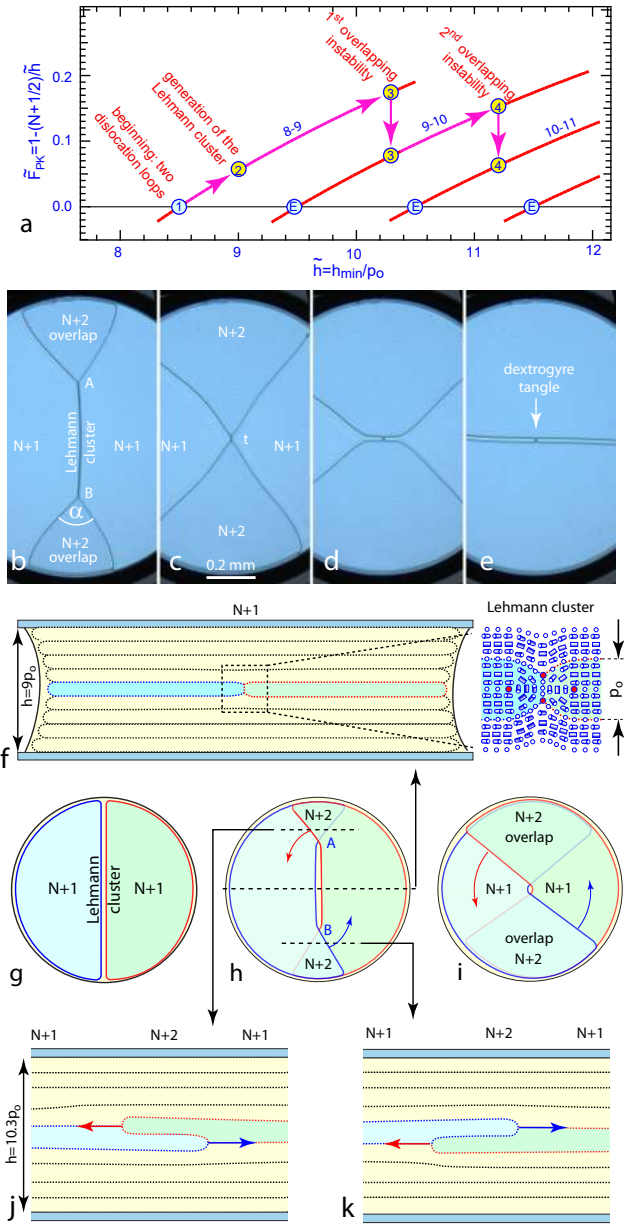


FIGURE 2. Generation of one dextrogyre tangle of dislocations from the Lehmann cluster in a droplet with $N=8$ cholesteric pitches. a) Variation of the Peach Koehler force with the thickness of the gap. b-e) 1st overlapping instability occurring at $\tilde{h} = 10.3$. f) Cross section of the droplet with the Lehmann cluster. g-i) Top views of the droplet during the generation of the tangle. j-k) Cross sections of the two types of N+2 overlaps. (0.87% CB15/5CB, $N=8$, $p_o = 18\mu m$).

One could think that this collision should result in coalescence of the two triangular fields. Surprisingly, once again, this is not the case : in Figs.2b and h the vertices A and B remain in contact in the center t while the triangular fields continue to grow thanks to the motion of the delimiting dislocations.

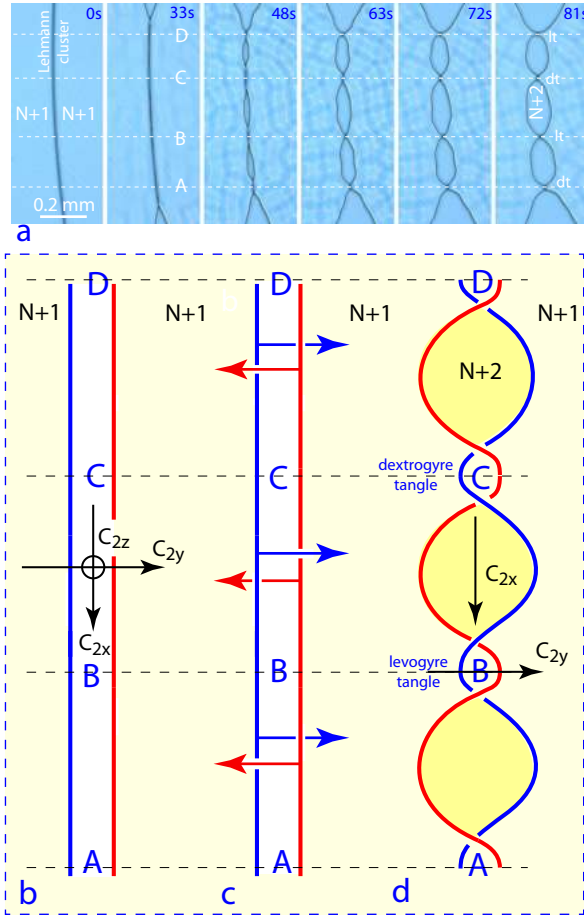


FIGURE 3. Tensile strain-induced generation of the levogyre and dextrogyre tangles (labeled “lt” and “dt”) by the overlapping instability of the Lehmann cluster. a) Temporal evolution as observed under a microscope (0.87% mixture of CB15 in 5CB, $p_o = 18\mu m$) : (0s)- pair of coplanar dislocations associated into the Lehmann cluster. (0s-81s)- the overlapping instability. b-d) Schematic representation of the 3D motions of dislocations that break the coplanar configuration of the Lehmann cluster and lead to generation of the tangles. C_{2x} , C_{2y} and C_{2z} are the two-fold axes of the D_2 symmetry group of the Lehmann cluster shown in (b).

This behaviour is the fingerprint of the metadefect - the *dextrogyre tangle of dislocations* - that appears as a black dot in Figs.2d and e.

To grasp better geometrical aspects of the generation of this tangle we show in Figs.2g-i top views of the droplet and in Figs.2j-k cross sections of the droplet along the dotted lines defined in Fig.2h. If the two cross sections were identical, for example such as the one in Fig.2j, the dislocation drawn in red would be located above the blue one everywhere. In this situation the red and blue dislocations would be free to expand until they would reach the meniscus of the cholesteric droplet. Therefore, the necessary condition for the generation of the tangle is that the two cross sections must be different : in Fig.2k,

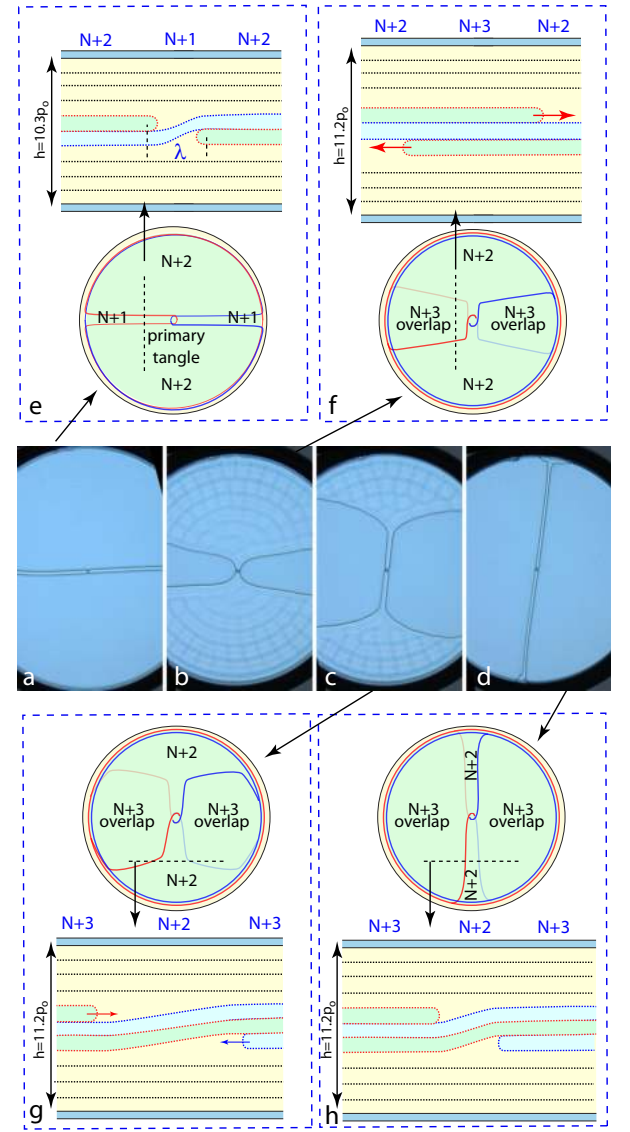


FIGURE 4. Beginning of the winding of a double-helix from the primary tangle. a-d) 2^{nd} overlapping instability (of a non coplanar dislocations pair) occurring at $\tilde{h} = 11.2$ (points 4 in Fig.2a). e-h) Structure of the cholesteric droplet during the 2^{nd} overlapping instability.

the dislocation drawn in red is located below the blue one.

These considerations lead us to examine the symmetry aspects of the generation of tangles using another example represented in Fig.3 in which not one but four tangles are generated simultaneously (see the video *Overlapping instability* in Supplementary Materials). Let us remark first that the Lehmann cluster has the D_2 symmetry containing three mutually orthogonal two-fold axes C_{2x} , C_{2y} and C_{2z} (see Fig.3b). Figs.3b-d show that the *overlapping instability* of the Lehmann cluster involving 3D motions of dislocations breaks its D_2 symmetry. After

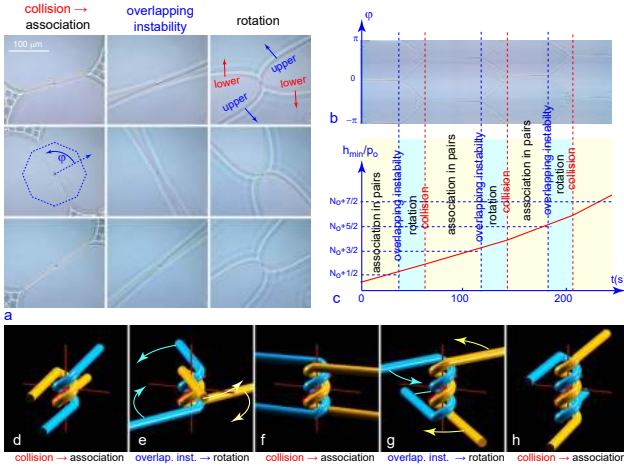


FIGURE 5. Winding of a dextrogyre double-helix tangle driven by a monotonic extension of the thickness \tilde{h} . a) Observations in a microscope. (5.4% mixture of CB15 in 5CB, $p_0 = 2.4\mu\text{m}$). b) Spatio-temporal cross section extracted from a video along the octagonal dashed line defined in (a). Staircase-like trajectories of dislocations in the spatio-temporal cross section are due to the thresholds to overcome during the successive overlapping instabilities. c) Growth of the reduced thickness in time. d-h) Perspective view of the winding process.

the $D_2 \rightarrow C_2$ symmetry breaking, only the two-fold axis C_{2x} is preserved. The four tangles of dislocations well visible in Fig.3a can now be seen as topological defects characteristic of the $D_2 \rightarrow C_2$ symmetry breaking.

Let us discuss in more details their genesis. In Fig.3b, the coplanar dislocation pair is divided by thought into three segments : AB, BC and CD. The red and blue arrows in Fig.3c indicate that in the AB and CD segments, the blue dislocation line passes below the red one while in the BC segment, it passes above the red one. The new configuration of dislocations in segments AB and CD are related to the one in BC by the broken symmetry elements C_{2y} and C_{2z} . Reconnection of the adjacent red (or blue) segments restores the continuity of the dislocation lines and generates the dextrogyre and levogyre tangles located alternatively in points A, B, C and D (see Fig.3d).

In experiments described above, the generation of the Lehmann cluster and its subsequent overlapping instability were driven by the Peach-Koehler forces acting on the red and blue segments of dislocations. The expression of the Peach-Koehler force in equation 2 depends on two dimensionless parameters : (1) the number N of cholesteric pitches in the confined droplet containing the dislocation loops, and (2) the reduced thickness of the droplet $\tilde{h} = h/p_0$. For this reason, for a given number N of the full cholesteric pitches ($N=8$), the generation of the Lehman cluster and the subsequent generation of tangles was obtained by the adequate variation of the droplet's dimensionless thickness represented in Fig.2a as a trajectory passing through points labeled from “1” to “3”.

1. At the beginning of our experiments, two dislocation loops were present in the droplet containing $N=8$ full cholesteric pitches (point 1 in Fig.2a).
2. The thickness \tilde{h} was then set to 9 (point 2 in Fig.2a), a value larger than 8.5, for which the Peach-Koehler force is positive so that the two dislocation converged, collided and the Lehmann cluster was formed (see Fig.1c).
3. With the aim to trigger the overlapping instability of the Lehmann cluster, \tilde{h} must be set to a value larger than 9.5, because after the instability the dislocation loops must continue their expansion in a droplet containing now $N=9$ pitches (see the line labeled 9-10 in Fig.2a). In practice, to get out from the energy well of depth $\Delta T = T_{LC} - 2T$ of the Lehmann cluster (the lowest energy state of a dislocation pair), the thickness was set to 10.3 (points 3 in Fig.2a), a value larger than 9.5. By this means the primary tangle of dislocations was generated.

When a solitary primary tangle is located in the centre of the droplet it is possible to wind it up into a double-helix tangle by a further extension of the gap thickness (see the videos *Double helix tangle* and *Perspective view of the double-helix tangle* in Supplementary Material). As the first example we show in Figs.4a-d continuation of the experiment from Fig.2b-e. Here, the primary tangle of dislocations obtained previously is submitted to the Peach Koehler forces corresponding to the thickness $\tilde{h} = 11.2$ (points 4 in Fig.2a) and the second overlapping transition occurs as shown in Figs.4e-h. Motion of dislocations (delimiting fields with $N+3$ pitches in Figs.4g and h) around the centre of the primary tangle increases the height of the tangle by p_0 .

In another experiment depicted in Fig.5, the growth of the thickness \tilde{h} is monotonic. In these conditions the sequence ... *collision* → *association in pairs* → *overlapping instability* → *rotation of dislocation* → *collision*... occurs several times and in this manner the primary tangle is wound up iteratively into a double-helix of a growing height. Let us stress that the staircase-like shape of trajectories of dislocations in the spatio temporal cross section in Fig.5b is due the thresholds that must be overcome during the successive overlapping instabilities of dislocation pairs. The perspectives views in Figs.5e-h simulate the winding process.

Our experiments opened several issues that deserve to be discussed in future in more details :

Immunity against the coalescence : Generation of the Lehmann cluster by the collision of two coplanar dislocation loops remains to be explained. It unveils a surprising immunity of coplanar dislocations against the coalescence (or rewiring).

The overlapping instabilities : The strain threshold $(\Delta\tilde{h}/\tilde{h})_{\text{crit}}$ necessary to get out from the potential well of the Lehmann cluster of depth $\Delta T = T_{\text{pair}} - 2T$ through the overlapping instability remains to be calculated.

Higher order tangles : When the winding process

starts from more complex networks of dislocations pairs containing several primary tangles, higher order tangles made of 3,...,8 dislocations can be wound up (see the video *Tangle six dislocations* in Supplementary Materials).

Geometry of helical tangles : The difference in geometries of the levogyre and dextrogyre double-helix tangles in CB15/5CB mixtures remains to be explained.

Networks of dislocation pairs : When several dislocation loops are nucleated and expand simultaneously, their collisions lead to formation of a foam-like polygonal network made of dislocation pairs connected by triple nodes. Due to tensions of dislocation pairs, this network evolves slowly like a foam. A much more rapid and complex reconfiguration of this network can be driven by a growing tensile strain. At the beginning, pairs of dislocations forming the Lehmann clusters may undergo the overlapping instability that generate primary tangles. In the subsequent evolution, the primary tangles can annihilate in pairs or associate into tangles of higher ranks (see below).

We would like to stress that other textures observed or discussed formerly in cholesterics can be seen as topological metadefects :

Kink chain generation in Lehmann clusters : Using optical tweezers and magnetic colloidal particles submitted to a rotating magnetic field, Varney, Jennes and Smalyukh [6] generated a series of kinks in a Lehmann cluster. The optical aspect of such a kink chain shown in Fig.8f of the ref.[6] is identical with that of an obliquely stretched double helix tangle observed in our studies (to be discussed elsewhere).

Dislocations in systems of twist-escaped disclination clusters : Using a computer controlled laser beam, patterns of twist-generated disclination clusters (cholesteric fingers) have been generated in thin cholesteric layers [11]. Dislocation in these systems of equidistant linear parallel clusters can also be seen as another type of metadefects, different from tangles.

Knotted dislocations and disclinations : The pos-

sibility of the occurrence of knotted dislocations generated in cholesterics confined between crossed mica sheets has been examined in ref.[12]. So far, closed dislocation loops, self-crossing several times, observed in experiments were topologically equivalent to the unknot. However, if the rewiring of some adequate crossings was possible (e.g. using heating by a laser beam), knots made of dislocations could be created. Generation of knots made of defect lines in nematics and their application in optics is extensively discussed in the recent paper of Meng, Wu and Smalyukh [13].

Finally, let us stress from the most general mathematical point of view, the association of the primary tangles obeys to a simple algebra involving their rank $t=n-1$ (where n is the number of entangled dislocations) and their levogyre and dextrogyre chiralities represented respectively, for example, by signs $-$ and $+$. Using this convention, the annihilation of a pair primary tangles is written as $1 - 1 = 0$ while the operation $1 + 1 + 1 = +3$ represents the association of three primary dextrogyre tangles into one dextrogyre tangle of rank $t=3$. It is also worthwhile to note that, in 5CB/CB15 mixtures, the director field in planes orthogonal to the double-helix levogyre and dextrogyre tangles contains respectively $+4\pi$ and -4π disclinations [8]. This fact is of interest for optical applications.

ACKNOWLEDGMENTS

This work on dislocations in cholesteric was initiated by the invitation of C.T. Imrie, R.D. Kamien and O.D. Lavrentovich for participation to the memorial issue of Liquid Crystals Reviews in honor of Maurice Kleman. We benefited from the technical assistance of V. Klein, Y. Simon, J. Sanchez, S. Saranga, J. Saen, T. Chambon, M. Bottineau, J. Vieira, and I. Nimaga. We are also grateful to C. Goldmann for discussions and help.

-
- [1] P.M. Chaikin and T. Lubensky, Principles of condensed matter physics, Cambridge University Press (2012).
 - [2] P.-G. de Gennes and J. Prost, The Physics of Liquid Crystals, Oxford University Press, Oxford (1993).
 - [3] O.D. Lavrentovich and D.K. Yang, Phys. Rev. E **57**, R6269–R6272 (1998).
 - [4] I.I. Smalyukh and O.D. Lavrentovich, Phys. Rev. E **66**, 051703-1–15 (2002).
 - [5] R.P. Trivedi, I.I. Klavets, B. Senyuk, T. Lee and I.I. Smalyukh, PNAS , 47441–4749 (2012).
 - [6] M.C.M. Varney, N.J. Jennes and I.I. Smalyukh, Phys. Rev. E , 022505-1–11 (2014).
 - [7] M. Kleman, J. Friedel, J. de Physique **30**, 555–654 (1969).
 - [8] Y. Bouligand, M. Kleman, J. de Physique **31**, 1041–1054 (1970).
 - [9] J. Rault, Sol. St. Com. **31**, 1041–1054 (1971).
 - [10] A. Darmon, M. Benzaquen, O. Dauchot and T. Lopez-Leon, PNAS **113** 9469-9474 (2016).
 - [11] P.J. Ackerman, Z. Qi, Y. Lin, C.T. Twombly, M.J. Laviada, Y. Lansac and I.I. Smalyukh, Scientific Reports **2**(1) 1–8 (2012).
 - [12] P. Pieranski and M.H Godinho, Liq. Cryst. 1–16 (2023).
 - [13] C. Meng, N.J. Jennes and I.I. Smalyukh, Nature Materials **22**, 64–72 (2023).